Cost-effective shrink of semi-critical layers using the TWINSCAN XT:1000H NA 0.93 KrF scanner

Frank Bornebroek[a], Marten de Wit[a], Wim de Boeij[a], Gerald Dicker[a], Jongkyun Hong[b], Alexander Serebryakov[a]

[a]ASML, De Run 6501, 5504 DR Veldhoven, The Netherlands
[b]ASML, No.59 Keji 6th Rd, Kuei-Shan, Taoyuan, Taiwan
Email Address: frank.bornebroek@asml.com
Phone: +31 40 268 3691

ABSTRACT

The TWINSCAN XT:1000H extends KrF lithography to expose layers that previously required more costly ArF lithography. These layers, including implants and metal interconnects, contain multiple, through pitch or random, 2-dimensional (2D) features.

In this paper, we show process windows for 115 nm random via holes using conventional illumination, 110 nm dense & isolated via holes using a soft quasar illumination shape, 95 nm trenches through pitch with an annular illumination mode as well as the process windows for a combination of patterns representative for implant structures using a soft annular illumination mode.

We also prove that the XT:1000H can be integrated in an existing high volume manufacturing environment: transfer of a 65 nm logic metal-1 layer from a high NA XT:1400 dry ArF scanner to the XT:1000H has been evaluated by optimizing the illumination settings and applying advanced mask design approaches to meet requirements for exposure latitude, depth of focus and MEEF. In addition, we show that the CD proximity matching performance between the XT:1000H and NA 0.8 XT:850 KrF scanners can be maximized using illumination setting optimization and EFESE focus scan. Finally, matched machine overlay performance between the XT:1000H and an XT:1900Gi ArF immersion scanner has been evaluated.

Keywords: KrF lithography, high NA, metal, via, implant, process transfer, proximity matching, matched overlay

1. INTRODUCTION

To reduce the lithography costs per wafer for future technology nodes, the TWINSCAN XT:1000H extends KrF lithography to expose layers that previously required more costly ArF lithography [1]. It can be used in high-volume manufacturing production of semi-critical layers in 65nm down to 22nm node applications. These layers include e.g. implants and metal interconnects.

The XT:1000H's NA 0.93 KrF projection lens enables KrF resolution extension to 80 nm and beyond. However, 80 nm resolution implies a k1 factor of 0.3 (with k1=resolution x NA / λ), which is typically only achievable for structures containing 1-dimensional (1D) dense lines and spaces. This allows for scanner illumination setting optimization for a single specific feature orientation or pitch range.

However, implant and metal interconnect layers, which, as mentioned above, will be the main application for the XT:1000H for future technology nodes can contain multiple, through pitch or random, 2-dimensional (2D) features. Examples are random via hole patterns, lines or trenches through pitch, which are typical for metal interconnects or a combination of features, which is typical for implant layers [2]. Such patterns need to be exposed using a more generic illumination condition to allow for all features to be printed simultaneously with a sufficiently large overlapping process window. The resolution limit or k1 factor for such patterns is therefore less aggressive. Previous reports show that the k1 limit for a pattern containing random via holes is about 0.4 [3]. This means that the XT:1000H system can potentially expose metal interconnect via layers down to 107 nm half pitch resolution.

Optical Microlithography XXII, edited by Harry J. Levinson, Mircea V. Dusa, Proc. of SPIE Vol. 7274, 72743I · © 2009 SPIE · CCC code: 0277-786X/09/$18 · doi: 10.1117/12.816521

In this paper, we will determine the process windows for 115 nm random via holes, 110 nm dense & isolated via holes, 95 nm trenches through pitch as well as a combination representative for implant structures of 120 nm dense lines, holes and 'islands', see Fig 1.

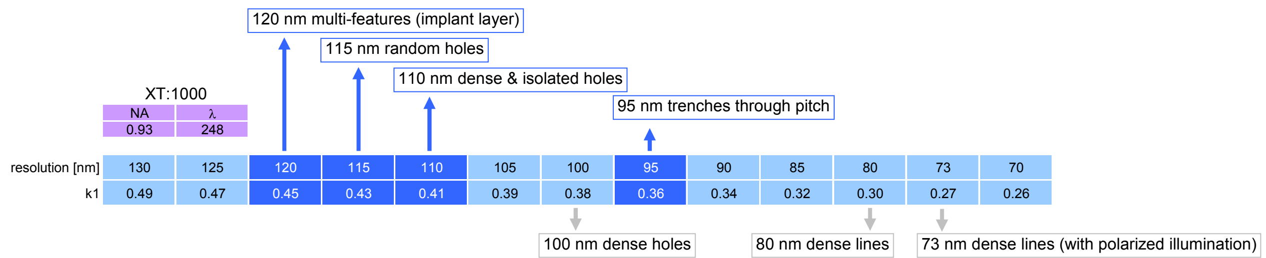

Fig 1 XT:1000H applications discussed in this paper (for dense applications at bottom see reference [1]).

Next to this enhanced imaging performance we will prove that the XT:1000H can be integrated in an existing high-volume manufacturing environment. This requires transferring an existing ArF process to KrF while still meeting the process window requirements, transferring layers from existing KrF scanners to the XT:1000H without changing process, mask or illumination setting and enabling matched overlay to immersion lithography systems below 10 nm.

2. ENHANCED KRF IMAGING PERFORMANCE

The XT:1000H illuminator supports advanced illumination modes created by means of Diffractive Optical Elements (DOE). Application of this DOE technique enables creation of imaging optimized illumination shapes without jeopardizing intensity or impacting throughput of the scanner, which is a requirement for implementation in high volume IC manufacturing. Stretching the resolution limit for multi-pitch via hole applications to k1~0.4 by using bull's eye or soft quasar illumination shapes – which combine an annular ring or poles with a small conventional area and are known to be optimal for such applications – becomes therefore practical.

2.1 115 nm random via hole imaging

To explore the random via holes printing capability of the XT:1000H, we have assumed a random via hole pattern as depicted in Fig 2. We have limited our analysis to a selection of representative holes, numbered 1-6 in this figure. We have found that a 6% att. phase shift mask in combination with conventional illumination yielded the best overall process window performance, with the least effort in mask optical proximity corrections (OPC). The mask shown in Fig 2 already includes OPC.

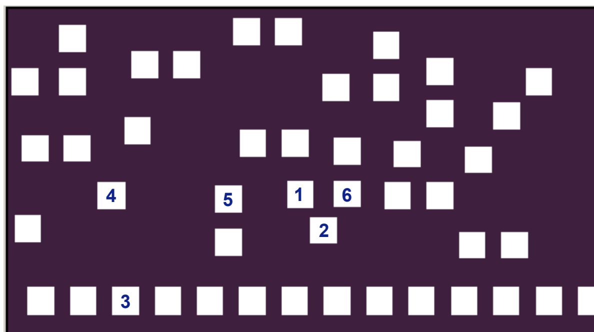

Fig 2 Random via hole pattern on mask. The critical via holes are labeled 1-6.

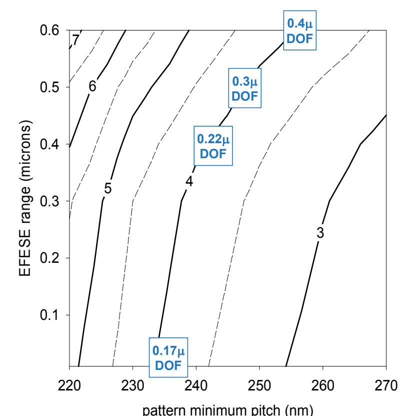

Fig 3 MEEF as function of minimum pitch and EFESE focus scan. The associated DOF values for MEEF=4 are indicated.

The most critical pitches required usage of the maximum NA of 0.93, in combination with a large partial coherence factor of 0.80. Because of this high NA, the DOF of the more isolated features can become critical. This can be compensated for by introducing focus scan movement (EFESE). However, a focus scan inherently lowers image contrast and thus increases the mask error enhancement factor (MEEF). For volume manufacturing, a trade-off has to be found between maximum allowable MEEF and minimally required DOF. In Fig 3, the constraints on EFESE and critical pitch are shown for different MEEF values. For the critical MEEF value of 4.0, the gain in DOF is also included in this figure. It can be concluded that the minimum pitch of the random via hole pattern can be as small as 235 nm while meeting the MEEF requirement. The expected depth of focus is ~170 nm in that case.

For the via hole pattern process window experimental verification, we have chosen 230 nm as the critical pitch. The resist stack was identical to the 110 nm dense and isolated via holes experiment, see 2.2. In Fig 4 the depicted process window shows a maximum depth of focus of 200nm and a maximum exposure latitude of 14%. MEEF values are in the 3.5-3.8 range, which is acceptable for random via applications. Fig 5 depicts the resist images through focus.

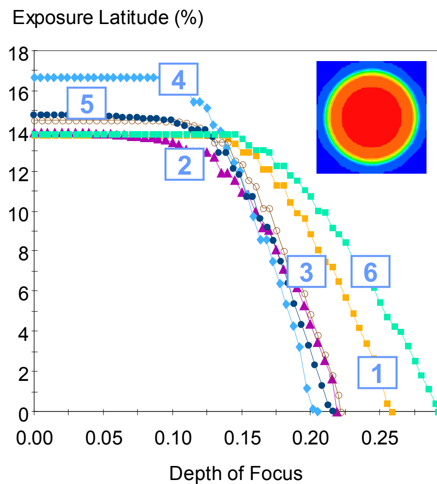

Fig 4 115 nm random via hole process window for features 1-6.

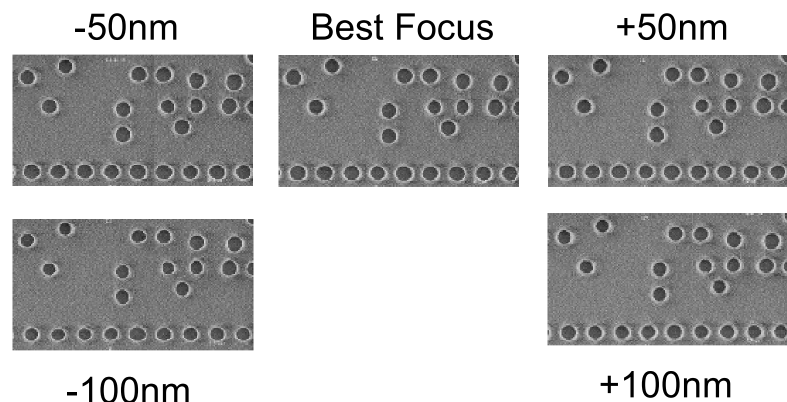

Fig 5 115 nm random via hole patterns in resist through focus.

To explore the XT:1000H printing limits of random via hole patterns, the process window has been simulated for minimum half-pitches smaller than 115nm now using a soft quasar illumination mode which is optimal for imaging of dense and isolated via holes simultaneously, see [3]. In Fig 6 and Fig 7 the simulated process windows for 100 nm & 107 nm random via holes are shown.

For the 100 nm case, the used soft-annular illumination setting was NA 0.93, poles $\sigma_{inner}/\ \sigma_{outer} = 0.78/0.97$, conventional $\sigma_{outer} = 0.4$ (with intensity balance between annular ring and conventional part of 1: 0.8), mask 6% att-PSM and 25nm bias. The maximum depth of focus of 150 nm and maximum exposure latitude of ~7% are small. Additionally, the MEEF for individual via holes ranges from 6.6 to 8.7.

For the 107 nm case, the used soft-annular illumination setting was NA 0.93, poles $\sigma_{inner}/\ \sigma_{outer} = 0.75/0.95$; conventional $\sigma_{outer} = 0.4$, mask 6% Att-PSM and 23nm bias. The maximum depth of focus of 160 nm and maximum exposure latitude of 9.5% seem feasible for high volume manufacturing. However, the MEEF for individual via holes ranges from 5.0 to 6.1, where for this application a maximum MEEF of 4 is required for high volume manufacturing.

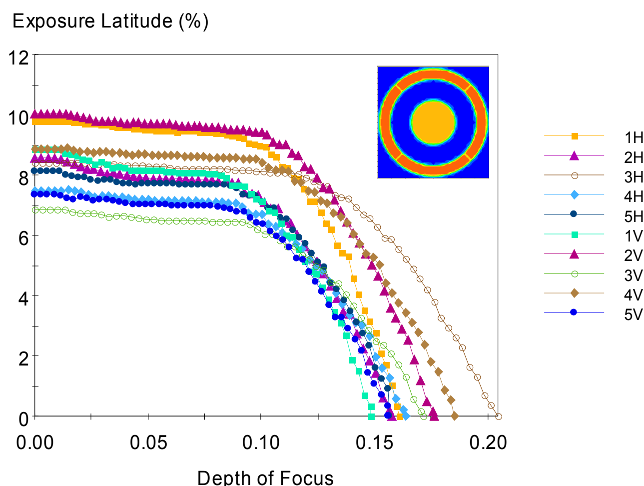

Fig 6 100 nm random via hole process window for features 1-5.

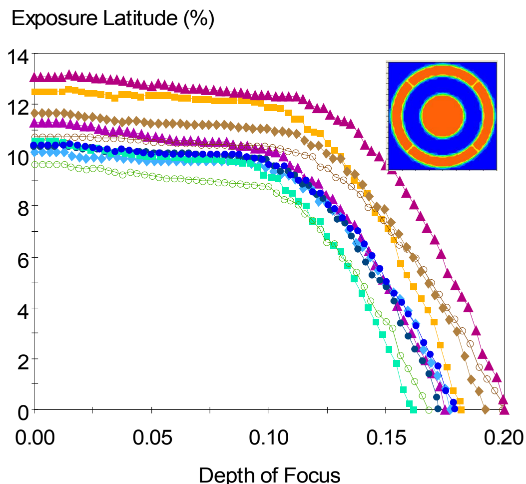

Fig 7 107 nm random via hole process window for features 1-5.

This means that the critical pitch of a random via holes pattern needs to be relaxed to values larger than 214 nm. Alternatively, limiting the pitch range to dense and isolated only, which can be feasible for specific applications, also enlarges the process window. Therefore, to verify the application of soft quasar illumination modes in the next section the XT:1000H printing capability of 110 nm dense and isolated via holes has been evaluated.

2.2 110 nm Dense & Isolated via holes

Previous KrF systems with an NA=0.8 are known to be capable of simultaneously printing 130~150nm via holes at multiple pitches. Here, we will show the benefit of the larger NA of the XT:1000H projection lens by verifying the process window for 110 nm dense and isolated via holes.

A soft quasar illumination mode which maximizes the overlapping process window has been applied. The ring width of the poles with a 20 degree opening angle is fixed at 0.20. Larger poles will decrease the process window since part of the 1st diffraction orders will fall outside the pupil. The NA is set at 0.93, because the diffraction orders for the 110nm dense via holes are partially blocked for NA<0.90. Optimizing the dense holes for contrast and the isolated holes for depth of focus, the illumination mode has been determined as: NA = 0.93; soft-quasar 20 degrees; poles σ_{inner}/ σ_{outer} = 0.73/0.9; conventional σ_{outer} = 0.20, see Fig 8.

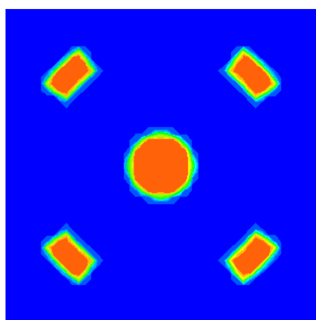

Fig 8 Optimal soft quasar illumination mode for 110 nm dense and isolated via hole printing.

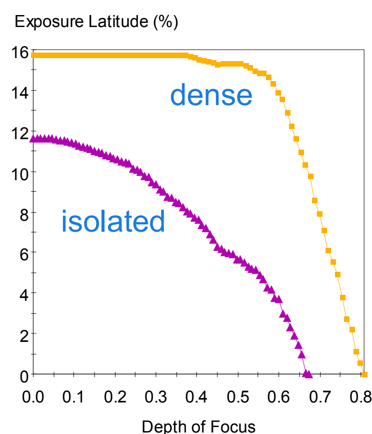

Fig 9 Measured process window of 110 nm dense & isolated via holes .

With this setting the process window has been verified on the XT:1000H using the following resist stack: 60 nm DUV46 (BARC); 275 nm GKR-5315 E8 (resist): 57nm Aquatar 8 (topcoat). From Fig 9 it appears that maximum exposure latitude of 11% and maximum depth of focus of 650 nm can be achieved, which is sufficient for high-volume manufacturing.

2.3 95 nm through pitch trenches

Interconnect metal layers typically consist of lines and spaces through pitch. In the case of a Cu damascene process trenches are exposed rather than lines. Here, we show the printing capabilities of the XT:1000H for 95 nm horizontal and vertical trenches through pitch which can be represented by a minimum k1 of 0.356 at a maximum NA of 0.93.

Fig 10 shows the through pitch trenches exposed at best focus. Assist features have been applied to the trenches at pitches 1:3 and 1:6 to enhance the common process window. Process conditions for these exposures were: NA=0.93, annular illumination with σ_{inner} = 0.66 and σ_{outer} = 0.81; Resist stack: 60 nm DUV46, 330 nm PEK500 and 57nm Aquatar 8.

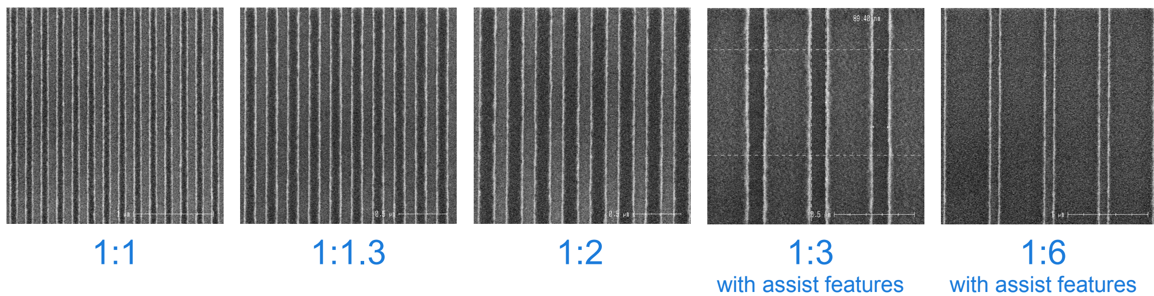

Fig 10 95 nm through pitch trench patterns in resist at best focus.

A common process window as depicted in Fig 11 has been achieved of >7% exposure latitude and >150 nm depth of focus. In Fig 12 one can also see that the depth of focus is limited by the isolated features whereas the exposure latitude is limited by the trenches at a 1:2 pitch that does not allow for assist features to enhance the process window.

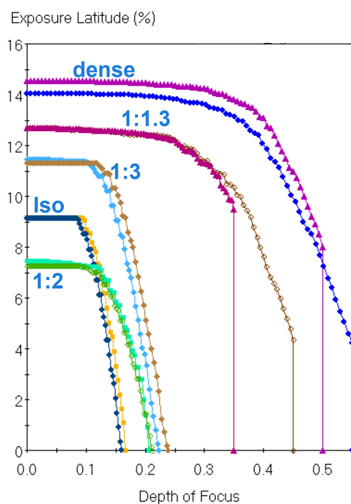

Fig 11 95 nm through pitch (horizontal and vertical) trenches process windows.

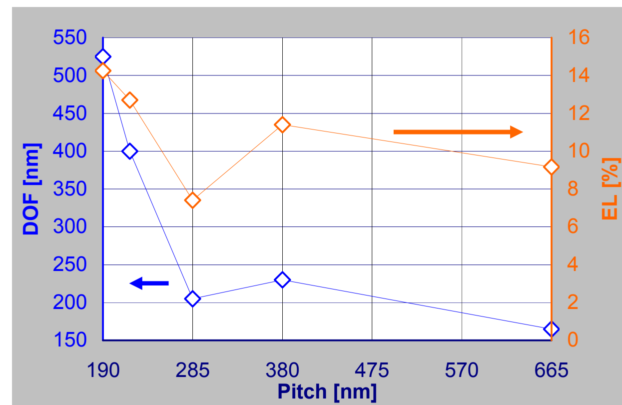

Fig 12 Depth-of-focus and exposure latitude as function of pitch for 95 nm trenches .

2.4 Multi feature printing

Finally, to validate the XT:1000H for implant layer applications, we have taken the approach to simultaneously print multiple structures and verify the overlapping process window, as has been done earlier for ArF lithography [2]. In that paper, dense lines were combined with holes and islands at a more relaxed pitch. To verify the printing limit of the XT:1000H for such combined structures, here we combined dense lines, holes and islands all at the *same* half pitch of 120 nm (k1=0.45) which is more aggressive than can be expected for typical implant layers. In Fig 13 all features in resist exposed in best focus have been depicted. A soft annular illumination mode has been used (see Fig 13 (right hand side)) for a balanced optimization of the process windows for the individual structures: NA = 0.93; annular σ_{inner} = 0.75 and σ_{outer} = 0.90; conventional σ_{outer} = 0.40 and the following resist stack: 60 nm DUV46, 225 nm PEK500, 57nm Aquatar 8.

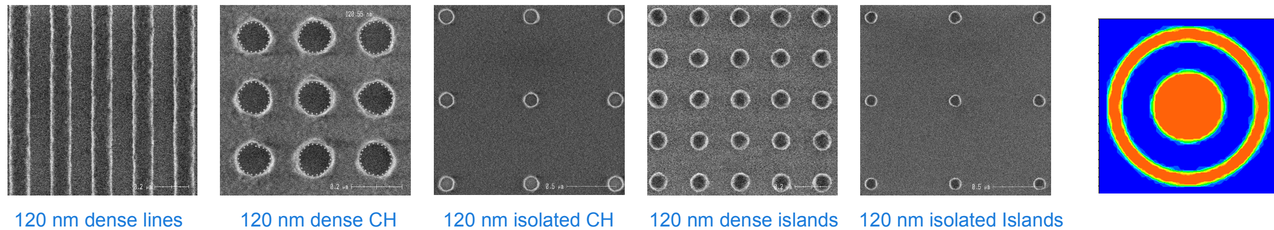

Fig 13 120 nm structures simultaneously exposed in best focus using a soft annular illumination mode.

In Fig 14, Fig 15 and Fig 16 the process windows for the individual structures are depicted. The dense lines show a very large process window with >300 nm depth of focus and >17% maximum exposure. The holes show a process window with maximum depth of focus >200 nm and maximum exposure latitude >14%. Also the dense islands show an appropriate process window with maximum depth of focus >150nm and maximum exposure latitude >15%. Most critical feature among all is the isolated island that in spite of it's large exposure latitude exhibits a small depth of focus of 100 nm.

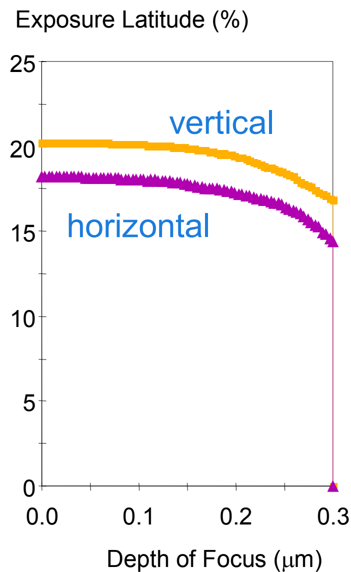

Fig 14 120 nm dense lines.

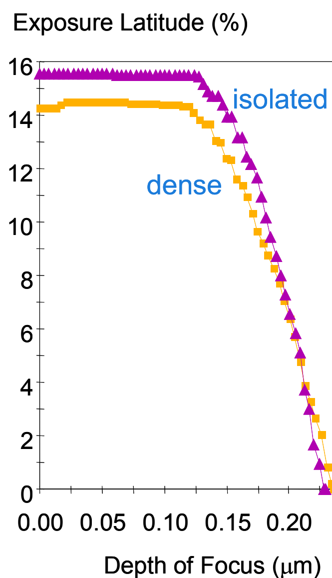

Fig 15 120 nm holes.

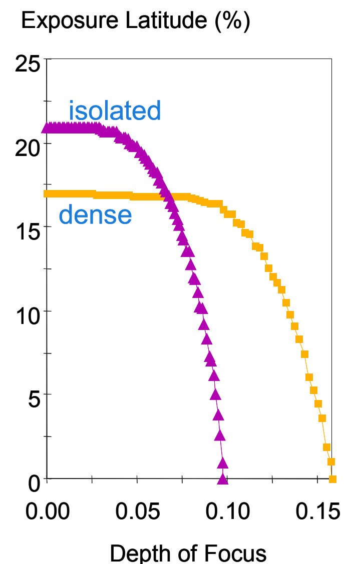

Fig 16 120 nm islands.

It appears that at negative focus (wafer moving away from projection lens) the bottom part of the islands becomes too small to support the island, leading to pattern collapse, see Fig 17. The larger process window for 130 nm islands in Fig 18 shows that increasing the size of the isolated island improves the process window.

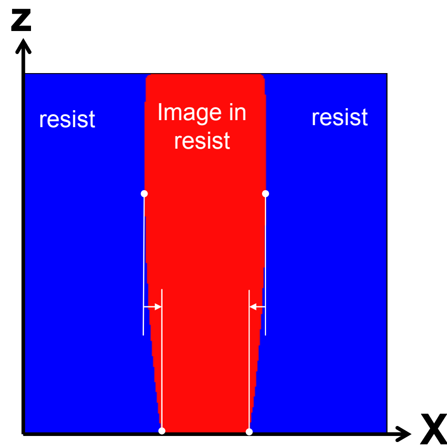

Fig 17 Simulated cross section of island pattern showing the tapered bottom leading to pattern collapse at negative defocus

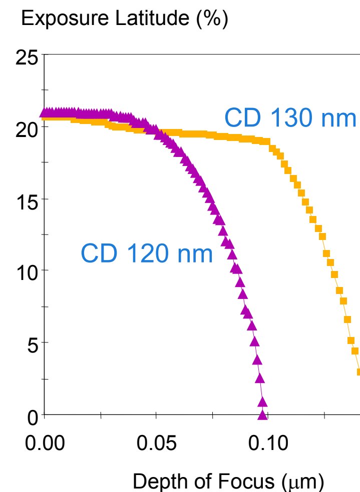

Fig 18 120 nm and 130 nm isolated islands process windows.

3. IMPLEMENTATION IN HIGH VOLUME MANUFACTURING

To implement the XT:1000H in a volume manufacturing environment, apart from process window requirements, several other critical aspects need to be assessed as well. To benefit from its lower cost per wafer, candidate ArF processes need to be transferred to KrF. This implies optimizing the illumination condition, verifying the KrF resist performance and potentially applying some kind of OPC to the mask design. In this section we will discuss this ArF to KrF process transfer feasibility of 100 nm lines through pitch that are typical for a 65 nm logic metal layer layout.

Secondly, to optimize manufacturing flexibility covering multiple products at multiple technology nodes in a single fab, it may be required to also transfer layers form existing KrF scanners. We will show that the XT:1000H can expose layers already qualified on previous generation KrF scanners (TWINSCAN XT:850) without changes to mask (proximity effects) or illumination setting.

Thirdly, main applications for the XT:1000H are implant or interconnect layers. For these layers, excellent overlay to critical front-end layers, which are exposed using ArF immersion technology, is prerequisite. Therefore, we will discuss the matched overlay performance between the XT:1000H and a TWINSCAN XT:1900Gi ArF immersion scanner.

3.1 Lithography process transfer from ArF to KrF

Transfer of a 65 nm logic metal layer (100 nm half-pitch) typically running on a high NA dry ArF scanner (XT:1400) to the XT:1000H has been evaluated by optimizing the illumination settings and applying advanced mask design approaches to meet volume manufacturing requirements for exposure latitude, depth of focus and MEEF

The following evaluation method has been applied using LithoCruiser™ (with NA/sigma optimizer and rule based OPC modules) assuming a 6% attenuated phase shift mask:

1. Check reference (ArF) process capability and select characteristic features to determine 'weak' points within layout of mask design indicating critical contrast values that can cause imaging challenges.
2. Optimize the (KrF) illumination setting and mask design with process window boundaries that satisfy the specification.
3. Qualify the process transfer feasibility by comparing process performance on the reference and target scanner with overlapping process window and MEEF.

Using a relevant production exposure setting at the ArF system, the reference process windows for CD through pitch reference structures have been simulated (see Fig 19). It shows a common process window for the metal layer of 15% exposure latitude with 250nm depth of focus. Since CD proximity effects change through pitch, five characteristic metal layer features have been selected ranging from dense to isolated, see Fig 20. These are used for optimizing the illumination setting and mask design.

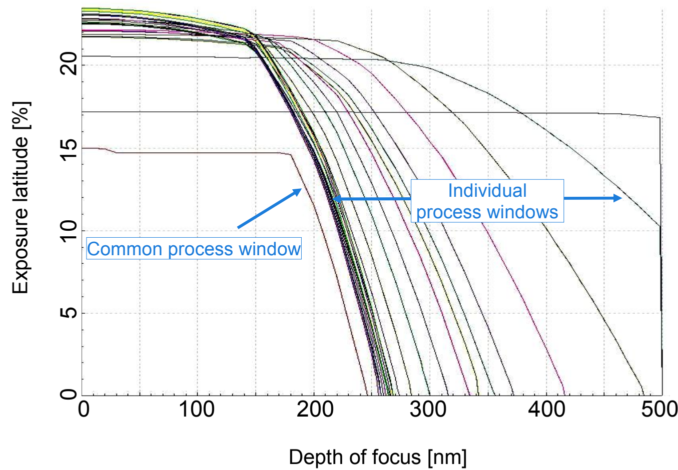

Fig 19 Reference ArF process window for the metal layer.

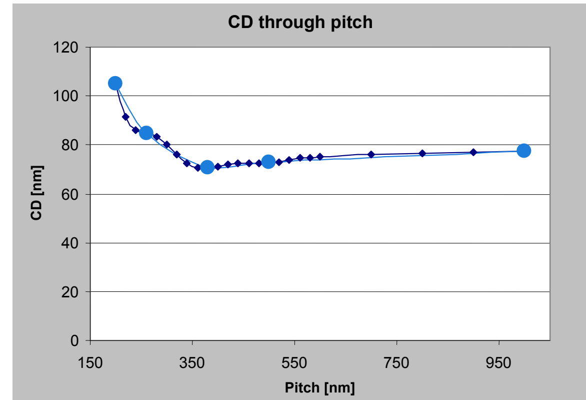

Fig 20 CD through pitch curve with characteristic features (large dots) .

Next, the illumination setting has been optimized for maximizing overlapping process window with the mask design as shown in Fig 21. As a result, an annular illumination mode has been recommended for the metal layer. With help of the automatic rule-based OPC optimization module in LithoCruiser^{TM}, the mask CD bias and also assisting feature rules have been optimized for improving process window for the specific illumination setting. In Fig 21 we show the resulting assisting features between the lines.

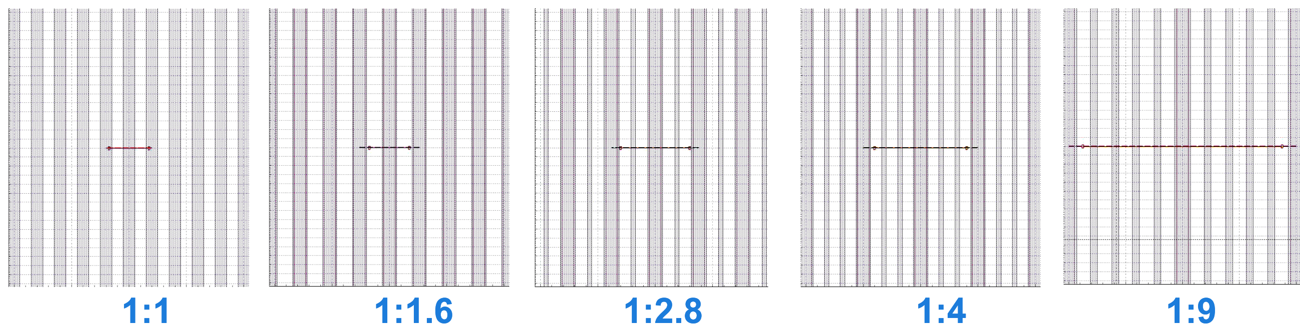

Fig 21 Metal layer mask design optimizing result including bias and assist features.

Subsequent simulations show that the maximum common KrF process window for the metal layer is 12% exposure latitude with 300nm of depth of focus. We can see that the dense feature limits the exposure latitude and isolated feature limits the depth of focus, as shown in Fig 22.

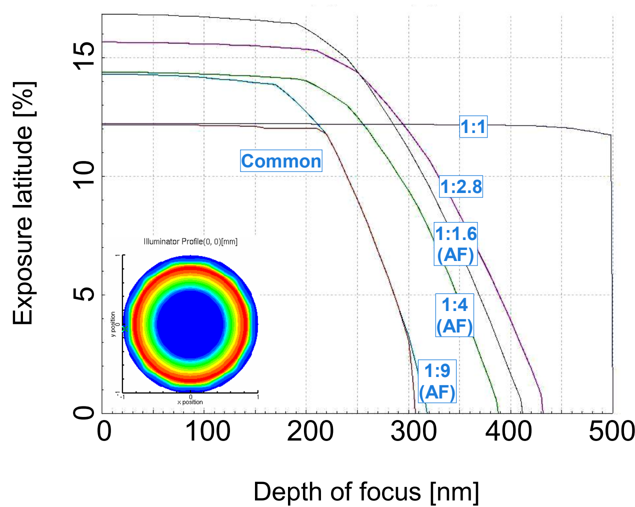

Fig 22 Optimized KrF process window for the metal layer using an annular illumination mode.

Finally, to qualify process transfer feasibility, a comparison between the ArF and KrF overlapping process windows has been made, as shown in Fig 23. The KrF process window in terms of maximum exposure latitude decreases by about 3%, but is still acceptable for production being well above 10%. The maximum depth of focus of KrF process for the metal layer is even larger than for the reference ArF process.

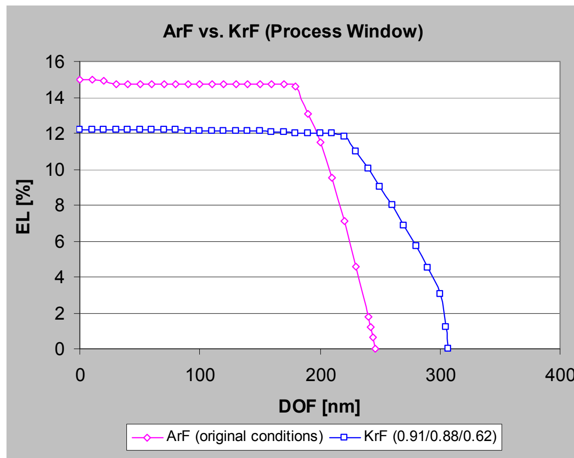

Fig 23 Common process window comparison between ArF and KrF processes for the metal layer.

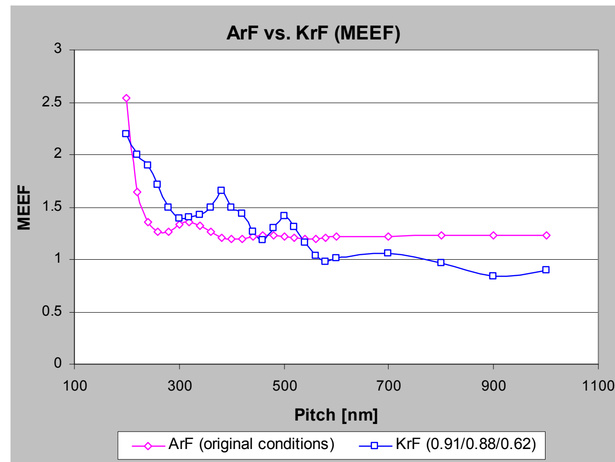

Fig 24 MEEF comparing ArF to KrF for the metal layer.

In addition, CD uniformity control is one of the key items for the process transfer feasibility. Therefore, MEEF values through pitch have been investigated and are shown in Fig 24. The maximum MEEF value of KrF process shows a value of 2.2 and is equivalent to the ArF process.

By optimizing the illumination setting and applying advanced OPC solution, we have obtained an overlapping process window of critical metal layer features for the KrF process that is comparable to the original ArF process. The good MEEF performance also allows for stable CD uniformity control within a broad line through pitch range.

3.2 XT:1000H CD matching to an NA 0.8 TWINSCAN XT:850 system

The CD proximity matching performance between the XT:1000H and an NA 0.8 XT:850 scanner has been verified by exposing 110 nm lines through pitch at both scanners using the same mask, annular illumination setting and resist process. In Fig 25 XT:1000H proximity curves and offsets have been plotted and compared to the population of proximity curves of 15 XT:850 systems.

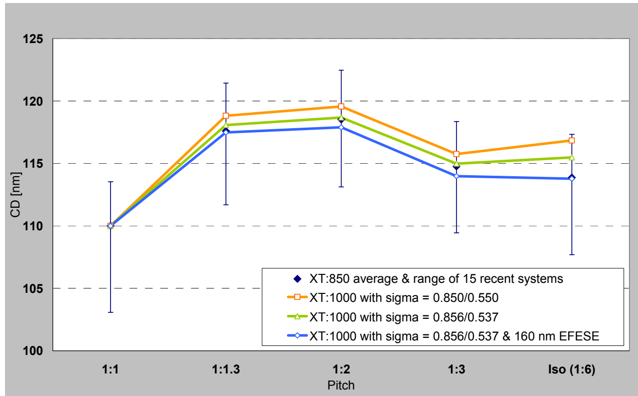

Fig 25 CD of 110 nm lines through pitch with XT:850 population results for 3 imaging conditions.

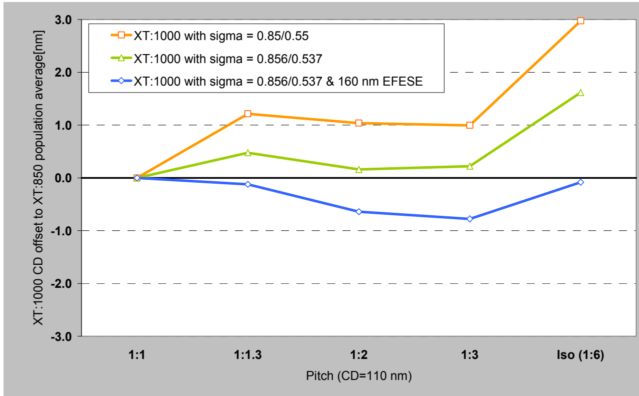

Fig 26 CD offset between XT:1000H and XT:850 population average.

By applying identical illumination settings to both scanner types, the XT:1000H proximity curve falls within the XT:850 population. The maximum offset between the XT:1000H and the XT:850 population average is ~3 nm, which is adequate for this resolution.

To improve the proximity matching performance, the XT:1000H illumination setting can be calibrated to the measured XT:850 average pupil with $\sigma_{inner} = 0.537$ and $\sigma_{outer} = 0.856$. With this illumination setting the proximity offset is reduced to < 2nm, see Fig 26. Even further optimization is possible using the EFESE focus scan. This method can be applied to compensate for residual contrast differences between scanner types. Applying a focus scan of 160 nm leads to a proximity offset < 1 nm, see also Fig 26.

From these results, it can be concluded that applications running on an XT:850 can be transferred to the XT:1000H without changes to illumination setting or mask OPC. Illumination setting calibration and EFESE can further enhance the proximity matching performance to sub-nm levels.

3.3 Matched overlay to an immersion scanner

For the 45nm technology node and beyond, critical layers will be exposed using ArF immersion scanners. For semi-critical layers like implants and interconnects that are being exposed using the XT:1000H, accurate overlay to these critical layers is required. Since for implant layers the overlay requirements can be as small as 12 nm, matched machine overlay between the XT:1000H and an ArF immersion scanner should be below 10 nm.

To prove that the XT:1000H is capable to meet these tight requirements, we have verified the matched overlay performance between the XT:1000H and an XT:1900Gi ArF immersion scanner following the standard calibration and verification methods. First, both wafer stage chucks have been matched per scanner using the two-dimensional exposure (2DE) grid calibration method. With this method, the residual grid fingerprint of each chuck is matched to the grid of a reference wafer. Resulting grid corrections are automatically applied during wafer exposure, independent of field size and wafer layout. Next, a first layer has been exposed on 10 wafers on the XT:1900Gi and subsequently etched in silicon. After this, a second layer has been exposed on 2 wafers on the XT:1000H. Based on the overlay results of these 2 wafers both scanners have been matched by applying linear inter and intra field process corrections. Finally, a 2nd layer has been exposed on the remaining 8 wafers and overlay has been measured using the scanner alignment system.

In Fig 27 the XT:1000H overlay results matched to an XT:1900Gi have been plotted for each of the 8 wafers. Here we applied the standard ASML overlay measurement method that includes 44 fields. In Fig 28 the wafer plot represents the lot average with full lot overlay (99.7% of pooled data) equal to (5.7, 5.2) nm for the x and y directions.

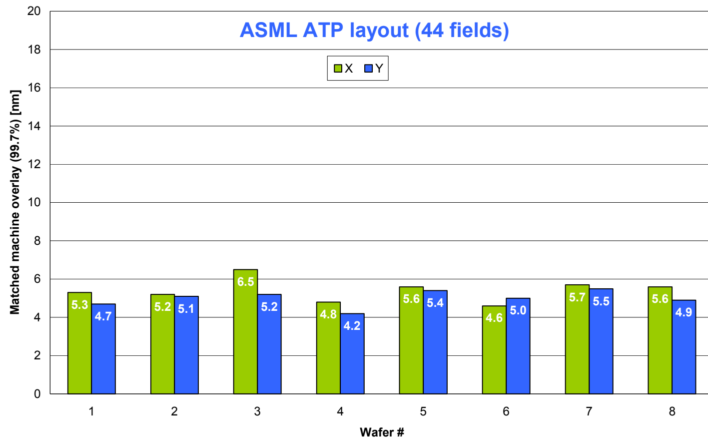

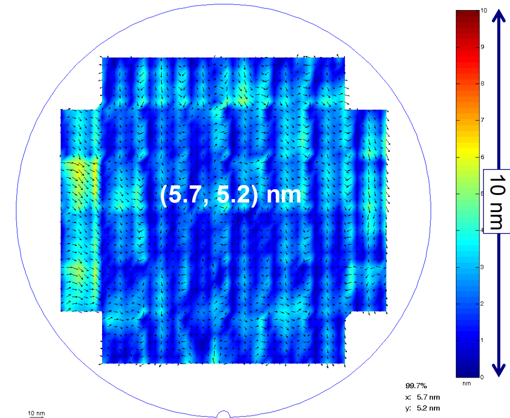

Fig 27 XT:1000H to XT:1900Gi overlay (8 wafers, 44 fields per wafer, 49 points per field, 99.7%).

Fig 28 XT:1000H to XT:1900Gi matched overlay average wafer plot with lot overlay based on pooled results from all 8 wafers (44 fields per wafer, 49 points per field, 99.7%).

In addition to the reduced inner wafer layout, we also measured the full wafer matched overlay increasing number of field during overlay measurements to 68 fields. In Fig 29 the XT:1000H full wafer overlay results matched to an XT:1900Gi have been plotted for each of the 8 wafers. The wafer plot in Fig 30 represents the lot average with full lot overlay (99.7% of pooled data) equal to (6.1, 6.1) nm for the x and y directions.

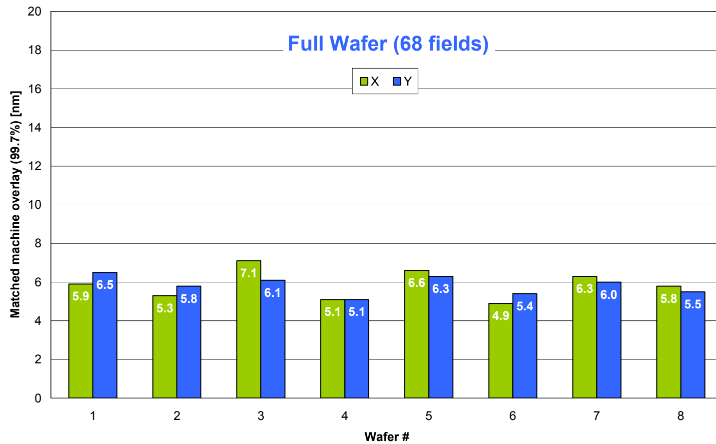

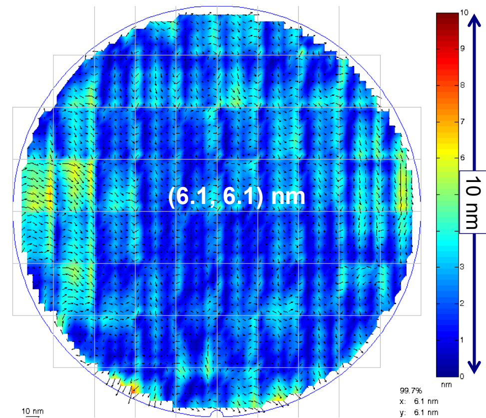

Fig 29 XT:1000H to XT:1900Gi matched overlay (8 wafers, 68 fields per wafer, 49 points per field, 99.7%).

Fig 30 XT:1000H to XT:1900Gi matched overlay average wafer plot with lot overlay based on pooled data from all 8 wafers (68 fields per wafer, 49 points per field, 99.7%).

These results show the excellent matched overlay capability of the XT:1000H specific and advanced TWINSCAN systems in general proving that future overlay requirements for XT:1000H applications can be met.

The authors would like to thank Anita Bouma, Remco Groeneveld, Steve Hansen, Joep van Dijk, Kees Ricken, Yin Fong Choi, Elliott McNamara and Bart Paarhuis for their contributions to this paper.

REFERENCES

[1] Wim de Boeij at al., "Extending KrF lithography beyond 80nm with the TWINSCAN XT:1000H 0.93NA scanner", Proc. SPIE Vol. 7140, 71401B (2008)

[2] D.C. OweYang et al., "Process Improvements by Applying 193 nm Lithography to 90 nm Logic Implant Layers", Proc. SPIE, Vol. 5038, 1095 (2003)

[3] Jo Finders et al., "Experimental evaluation of Bulls-Eye illumination for assist-free, random contact printing at sub-65nm node", Proc. SPIE, Vol. 6154, 615412 (2006)